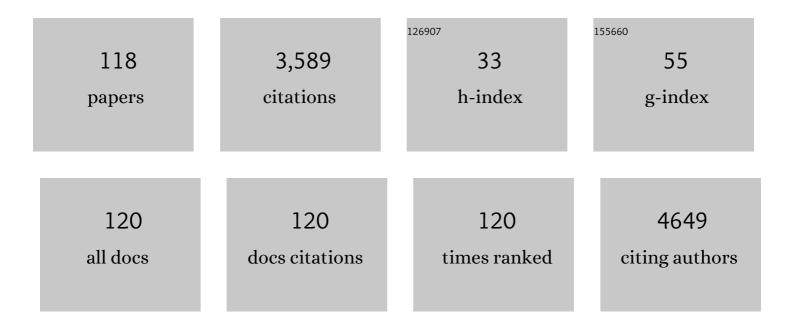
Shanming Ke

List of Publications by Year in descending order

Source: https://exaly.com/author-pdf/8714671/publications.pdf Version: 2024-02-01



| # | Article | IF | CITATIONS |
|----|--|------|-----------|
| 1 | Giant Electric Energy Density in Epitaxial Leadâ€Free Thin Films with Coexistence of Ferroelectrics and Antiferroelectrics. Advanced Electronic Materials, 2015, 1, 1500052. | 5.1 | 195 |
| 2 | Large Energy Storage Density and High Thermal Stability in a Highly Textured (111)-Oriented Pb _{0.8} Ba _{0.2} ZrO ₃ Relaxor Thin Film with the Coexistence of Antiferroelectric and Ferroelectric Phases. ACS Applied Materials & Interfaces, 2015, 7, 13512-13517. | 8.0 | 185 |
| 3 | Ferroelectricâ€Enhanced Polysulfide Trapping for Lithium–Sulfur Battery Improvement. Advanced Materials, 2017, 29, 1604724. | 21.0 | 149 |
| 4 | Photoflexoelectric effect in halide perovskites. Nature Materials, 2020, 19, 605-609. | 27.5 | 132 |
| 5 | Relaxor behavior in CaCu3Ti4O12 ceramics. Applied Physics Letters, 2006, 89, 182904. | 3.3 | 128 |
| 6 | Vibration catalysis of eco-friendly Na0.5K0.5NbO3-based piezoelectric: An efficient phase boundary catalyst. Applied Catalysis B: Environmental, 2020, 279, 119353. | 20.2 | 128 |
| 7 | Flexoelectric materials and their related applications: A focused review. Journal of Advanced Ceramics, 2019, 8, 153-173. | 17.4 | 127 |
| 8 | Lorentz-type relationship of the temperature dependent dielectric permittivity in ferroelectrics with diffuse phase transition. Applied Physics Letters, 2008, 93, . | 3.3 | 85 |
| 9 | Transparent Indium Tin Oxide Electrodes on Muscovite Mica for High-Temperature-Processed Flexible Optoelectronic Devices. ACS Applied Materials & Interfaces, 2016, 8, 28406-28411. | 8.0 | 83 |
| 10 | Black phosphorus quantum dots as dual-functional electron-selective materials for efficient plastic perovskite solar cells. Journal of Materials Chemistry A, 2018, 6, 8886-8894. | 10.3 | 80 |
| 11 | Effect of sintering temperature on the structure and properties of cerium-doped 0.94(Bi0.5Na0.5)TiO3–0.06BaTiO3 piezoelectric ceramics. Journal of Alloys and Compounds, 2008, 458, 504-508. | 5.5 | 78 |
| 12 | Dielectric relaxation in A2FeNbO6 (A = Ba, Sr, and Ca) perovskite ceramics. Journal of Electroceramics, 2009, 22, 252-256. | 2.0 | 75 |
| 13 | Antiferroelectric-like properties and enhanced polarization of Cu-doped K _{0.5} Na _{0.5} NbO ₃ piezoelectric ceramics. Applied Physics Letters, 2012, 101, 082901. | 3.3 | 71 |
| 14 | Panchromatic thin perovskite solar cells with broadband plasmonic absorption enhancement and efficient light scattering management by Au@Ag core-shell nanocuboids. Nano Energy, 2017, 41, 654-664. | 16.0 | 68 |
| 15 | Ionic liquid modified SnO ₂ nanocrystals as a robust electron transporting layer for efficient planar perovskite solar cells. Journal of Materials Chemistry A, 2018, 6, 22086-22095. | 10.3 | 66 |
| 16 | A giant negative electrocaloric effect in Eu-doped PbZrO ₃ thin films. Journal of Materials Chemistry C, 2016, 4, 3375-3378. | 5.5 | 62 |
| 17 | Facile fabrication of highly efficient ETL-free perovskite solar cells with 20% efficiency by defect passivation and interface engineering. Chemical Communications, 2019, 55, 2777-2780. | 4.1 | 61 |
| 18 | Ultrasonic vibration driven piezocatalytic activity of lead-free K0.5Na0.5NbO3 materials. Ceramics International, 2019, 45, 22486-22492. | 4.8 | 59 |

| # | Article | IF | CITATIONS |
|----|---|------|-----------|
| 19 | Dielectric dispersion behavior of Ba(ZrxTi1â^'x)O3 solid solutions with a quasiferroelectric state. Journal of Applied Physics, 2008, 104, . | 2.5 | 56 |
| 20 | Organic Photoâ€Electrochemical Transistorâ€Based Biosensor: A Proofâ€ofâ€Concept Study toward Highly Sensitive DNA Detection. Advanced Healthcare Materials, 2018, 7, e1800536. | 7.6 | 54 |
| 21 | Colossal dielectric response in barium iron niobate ceramics obtained by different precursors. Ceramics International, 2008, 34, 1059-1062. | 4.8 | 53 |
| 22 | Electrical modulus analysis on the Ni/CCTO/PVDF system near the percolation threshold. Journal Physics D: Applied Physics, 2011, 44, 475305. | 2.8 | 53 |
| 23 | Epitaxial array of Fe3O4 nanodots for high rate high capacity conversion type lithium ion batteries electrode with long cycling life. Nano Energy, 2020, 74, 104876. | 16.0 | 51 |
| 24 | Origin of Ferroelectricity in Epitaxial Si-Doped HfO ₂ Films. ACS Applied Materials & Interfaces, 2019, 11, 4139-4144. | 8.0 | 48 |
| 25 | High-Quality AZO/Au/AZO Sandwich Film with Ultralow Optical Loss and Resistivity for Transparent Flexible Electrodes. ACS Applied Materials & Interfaces, 2018, 10, 16160-16168. | 8.0 | 45 |
| 26 | TiO2/SiO2 hybrid nanomaterials: synthesis and variable UV-blocking properties. Journal of Sol-Gel Science and Technology, 2011, 58, 326-329. | 2.4 | 43 |
| 27 | van der Waals epitaxy of Al-doped ZnO film on mica as a flexible transparent heater with ultrafast thermal response. Applied Physics Letters, 2018, 112, . | 3.3 | 43 |
| 28 | Epitaxial ferroelectric Hf _{0.5} Zr _{0.5} O ₂ thin film on a buffered YSZ substrate through interface reaction. Journal of Materials Chemistry C, 2018, 6, 9224-9231. | 5.5 | 38 |
| 29 | Dielectric, ferroelectric properties, and grain growth of CaxBa1â ^{~3} xNb2O6 ceramics with tungsten-bronzes structure. Journal of Applied Physics, 2008, 104, . | 2.5 | 37 |
| 30 | Nearly constant dielectric loss behavior in poly(3-hydroxybutyrate- <i>co</i> -3-hydroxyvalerate) biodegradable polyester. Journal of Applied Physics, 2009, 105, . | 2.5 | 37 |
| 31 | Tuning of dielectric and ferroelectric properties in single phase BiFeO3 ceramics with controlled Fe2+/Fe3+ ratio. Ceramics International, 2014, 40, 5263-5268. | 4.8 | 36 |
| 32 | Structure, corrosion resistance and in vitro bioactivity of Ca and P containing TiO 2 coating fabricated on NiTi alloy by plasma electrolytic oxidation. Applied Surface Science, 2015, 356, 1234-1243. | 6.1 | 36 |
| 33 | Structural dependence of piezoelectric, dielectric and ferroelectric properties of K0.5Na0.5(Nb1â²²2/5Cu)O3 lead-free ceramics with high Q. Materials Research Bulletin, 2012, 47, 4472-4477. | 5.2 | 35 |
| 34 | Ferroelectric Polymer Thin Films for Organic Electronics. Journal of Nanomaterials, 2015, 2015, 1-14. | 2.7 | 35 |
| 35 | A novel and sensitive sarcosine biosensor based on organic electrochemical transistor. Electrochimica Acta, 2019, 307, 100-106. | 5.2 | 35 |
| 36 | Interfaces between hexagonal and cubic oxides and their structure alternatives. Nature Communications, 2017, 8, 1474. | 12.8 | 31 |

| # | Article | IF | CITATIONS |
|----|---|------|-----------|
| 37 | Revisit of the Vögel–Fulcher freezing in lead magnesium niobate relaxors. Applied Physics Letters, 2010, 97, 132905. | 3.3 | 30 |
| 38 | Variable-range-hopping conductivity in high-k Ba(Fe0.5Nb0.5)O3 ceramics. Journal of Applied Physics, 2013, 114, . | 2.5 | 30 |
| 39 | Crossover from a nearly constant loss to a superlinear power-law behavior in Mn-doped Bi(Mg1/2Ti1/2)O3–PbTiO3 ferroelectrics. Journal of Applied Physics, 2010, 107, . | 2.5 | 29 |
| 40 | Versatile and Highly Efficient Controls of Reversible Topotactic Metal–Insulator Transitions through Proton Intercalation. Advanced Functional Materials, 2019, 29, 1907072. | 14.9 | 28 |
| 41 | Use of a novel layered titanoniobate as an anode material for long cycle life sodium ion batteries. RSC Advances, 2016, 6, 35746-35750. | 3.6 | 27 |
| 42 | A sensitive DNA sensor based on an organic electrochemical transistor using a peptide nucleic acid-modified nanoporous gold gate electrode. RSC Advances, 2017, 7, 52118-52124. | 3.6 | 27 |
| 43 | Dielectric relaxation in polyimide nanofoamed films with low dielectric constant. Applied Physics Letters, 2008, 92, . | 3.3 | 25 |
| 44 | Structural and electric properties of barium strontium titanate based ceramic composite as a humidity sensor. Solid State Ionics, 2008, 179, 1632-1635. | 2.7 | 24 |
| 45 | Large nonlinear dielectric behavior in BaTi1â^'xSnxO3. Scientific Reports, 2017, 7, 6693. | 3.3 | 24 |
| 46 | Giant low frequency dielectric tunability in high-k Ba(Fe1/2Nb1/2)O3 ceramics at room temperature. Journal of Applied Physics, 2010, 108, 064104. | 2.5 | 23 |
| 47 | High dielectric tunability, electrostriction strain and electrocaloric strength at a tricritical point of tetragonal, rhombohedral and pseudocubic phases. Journal of Alloys and Compounds, 2015, 646, 597-602. | 5.5 | 23 |
| 48 | Large electrocaloric strength in the (100)-oriented relaxor ferroelectric Pb[(Ni1/3Nb2/3)0.6Ti0.4]O3 single crystal at near morphotropic phase boundary. Ceramics International, 2015, 41, 9344-9349. | 4.8 | 23 |
| 49 | Multichannel quartz crystal microbalance array: Fabrication, evaluation, application in biomarker detection. Analytical Biochemistry, 2016, 494, 85-92. | 2.4 | 23 |
| 50 | Flexoelectric behavior in PIN-PMN-PT single crystals over a wide temperature range. Applied Physics Letters, 2017, 111, . | 3.3 | 23 |
| 51 | Thermal-evaporated selenium as a hole-transporting material for planar perovskite solar cells. Solar Energy Materials and Solar Cells, 2018, 185, 130-135. | 6.2 | 22 |
| 52 | Giant dielectric response and enhanced thermal stability of multiferroic BiFeO3. Journal of Alloys and Compounds, 2014, 600, 118-124. | 5.5 | 21 |
| 53 | Effect of oxygen pressure on pulsed laser deposited WO3 thin films for photoelectrochemical water splitting. Journal of Alloys and Compounds, 2017, 722, 913-919. | 5.5 | 21 |
| 54 | Relaxor behavior and dielectric properties of lead magnesium niobate–lead titanate thick films prepared by electrophoresis deposition. Journal of Alloys and Compounds, 2009, 478, 853-857. | 5.5 | 19 |

| # | Article | IF | CITATIONS |
|----|---|------------|---|
| 55 | Performance of a building-integrated photovoltaic/thermal system under frame shadows. Energy and Buildings, 2017, 134, 71-79. | 6.7 | 19 |
| 56 | Efficient decomplexation of heavy metal-EDTA complexes by Co2+/peroxymonosulfate process: The critical role of replacement mechanism. Chemical Engineering Journal, 2020, 392, 123639. | 12.7 | 19 |
| 57 | Electric Polarization Switching on an Atomically Thin Metallic Oxide. Nano Letters, 2021, 21, 144-150. | 9.1 | 19 |
| 58 | Origin of colossal dielectric response in (In + Nb) co-doped TiO2 rutile ceramics: a potential electrothermal material. Scientific Reports, 2017, 7, 10144. | 3.3 | 18 |
| 59 | Atomic Steps Induce the Aligned Growth of Ice Crystals on Graphite Surfaces. Nano Letters, 2020, 20, 8112-8119. | 9.1 | 17 |
| 60 | Large flexoelectric response in PMN-PT ceramics through composition design. Applied Physics Letters, 2019, 115, . | 3.3 | 16 |
| 61 | Revisit of amorphous semiconductor InGaZnO4: A new electron transport material for perovskite solar cells. Journal of Alloys and Compounds, 2019, 789, 276-281. | 5.5 | 16 |
| 62 | Dielectric spectroscopy of biodegradable poly(3-hydroxybutyrate-co-3-hydroxyhexanoate) films. European Polymer Journal, 2012, 48, 79-85. | 5.4 | 15 |
| 63 | 1-Butyl-3-Methylimidazolium Tetrafluoroborate Film as a Highly Selective Sensing Material for Non-Invasive Detection of Acetone Using a Quartz Crystal Microbalance. Sensors, 2017, 17, 194. | 3.8 | 15 |
| 64 | Dielectric relaxations of high- <i>k</i> poly(butylene succinate) based all-organic nanocomposite films for capacitor applications. Journal of Materials Research, 2011, 26, 2493-2502. | 2.6 | 14 |
| 65 | Electrical and Dielectric Properties of Exfoliated Graphite/Polyimide Composite Films with Low Percolation Threshold. Journal of Electronic Materials, 2012, 41, 2439-2446. | 2.2 | 14 |
| 66 | Non-linear behavior of flexoelectricity. Applied Physics Letters, 2019, 115, . | 3.3 | 14 |
| 67 | Integration of a Miniature Quartz Crystal Microbalance with a Microfluidic Chip for Amyloid Beta-AÎ ² 42 Quantitation. Sensors, 2015, 15, 25746-25760. | 3.8 | 13 |
| 68 | Intrinsic and extrinsic effects on the ferroelectric switching of thin poly(vinylidene) Tj ETQq0 0 0 rgBT /Overlock | 10 Jf 50 2 | .22 ₁₃ ^T d (fluorid |
| 69 | Flexoelectric fatigue in (K,Na,Li)(Nb,Sb)O3 ceramics. Applied Physics Letters, 2018, 113, . | 3.3 | 13 |
| 70 | Modulation of Abnormal Poisson's Ratios and Electronic Properties in Mixed-Valence Perovskite Manganite Films. ACS Applied Materials & Interfaces, 2018, 10, 18029-18035. | 8.0 | 13 |
| 71 | Flexible TiO2/Au thin films with greatly enhanced photocurrents for photoelectrochemical water splitting. Journal of Alloys and Compounds, 2020, 815, 152471. | 5.5 | 13 |
| 72 | MgTiO3 doping effect on dielectric properties of Ba0.6Sr0.4TiO3 ceramics via a molten salt process. Composites Part A: Applied Science and Manufacturing, 2008, 39, 597-601. | 7.6 | 12 |

| # | Article | IF | CITATIONS |
|----|---|------|-----------|
| 73 | Dielectric and Thermal Properties of Polyimide–Poly(ethylene oxide) Nanofoamed Films. Journal of Electronic Materials, 2012, 41, 2281-2285. | 2.2 | 12 |
| 74 | Epitaxial ultrathin Au films on transparent mica with oxide wetting layer applied to organic light-emitting devices. Applied Physics Letters, 2019, 114, 081902. | 3.3 | 12 |
| 75 | Atomic-Scale insight into the reversibility of polar order in ultrathin epitaxial Nb:SrTiO3/BaTiO3 heterostructure and its implication to resistive switching. Acta Materialia, 2020, 188, 23-29. | 7.9 | 12 |
| 76 | Relaxor behavior and electrical properties of high dielectric constant materials. Science in China Series D: Earth Sciences, 2009, 52, 2180-2185. | 0.9 | 11 |
| 77 | A Novel Organic Electrochemical Transistor-Based Platform for Monitoring the Senescent Green Vegetative Phase of Haematococcus pluvialis Cells. Sensors, 2017, 17, 1997. | 3.8 | 11 |
| 78 | Electric modulation of conduction in MAPbBr3 single crystals. Journal of Advanced Ceramics, 2021, 10, 320-327. | 17.4 | 11 |
| 79 | Local structural heterogeneity induced large flexoelectricity in Sm-doped PMN–PT ceramics. Journal of Applied Physics, 2021, 129, . | 2.5 | 11 |
| 80 | Interplay of defect dipole and flexoelectricity in linear dielectrics. Scripta Materialia, 2022, 210, 114427. | 5.2 | 11 |
| 81 | Dielectric behaviors of PHBHHx–BaTiO3 multifunctional composite films. Composites Science and Technology, 2012, 72, 370-375. | 7.8 | 10 |
| 82 | Designing electron transporting layer for efficient perovskite solar cell by deliberating over nano-electrical conductivity. Solar Energy Materials and Solar Cells, 2019, 200, 109995. | 6.2 | 10 |
| 83 | Growth and properties of (1â^'x)Pb(Zn1/3Nb2/3)O3–xPbTiO3 (x=0.07–0.11) ferroelectric single crystals by a top-seeded solution growth method. Ceramics International, 2015, 41, 14427-14434. | 4.8 | 9 |
| 84 | Visualization of Bubble Nucleation and Growth Confined in 2D Flakes. Small, 2021, 17, e2103301. | 10.0 | 9 |
| 85 | Microstructure evolutions and electrical properties of Pb1â^'xLax(Zr0.56Ti0.44)1â^'x/4O3 ceramics. Materials Science and Engineering B: Solid-State Materials for Advanced Technology, 2007, 138, 205-209. | 3.5 | 8 |
| 86 | Structure and properties of PMN–PT/NZFO laminates and composites. Ceramics International, 2008, 34, 701-704. | 4.8 | 8 |
| 87 | Temperature-dependent reversible and irreversible processes in Nb-doped PbZrO3 relaxor ferroelectric thin films. Applied Physics Letters, 2015, 107, . | 3.3 | 8 |
| 88 | Synthesis of ferroelectric KNbO 3 nanosheets by liquid exfoliation of layered perovskite K 2 NbO 3 F. Journal of Alloys and Compounds, 2017, 698, 357-363. | 5.5 | 8 |
| 89 | Nano-electrical conductivity guided optimization of pulsed laser deposited ZnO electron transporting layer for efficient perovskite solar cell. Journal of Power Sources, 2020, 468, 228392. | 7.8 | 8 |
| 90 | Mean-Field Approach to Dielectric Relaxation in Giant Dielectric Constant Perovskite Ceramics. Journal of Ceramics, 2013, 2013, 1-7. | 0.9 | 8 |

| # | Article | IF | CITATIONS |
|-----|---|-----|-----------|
| 91 | Dielectric and ageing behaviour of strontium barium niobate with barium strontium titanate additives. Journal Physics D: Applied Physics, 2007, 40, 6797-6802. | 2.8 | 7 |
| 92 | Large increase of Curie temperature in (110)-oriented La0.7Sr0.3MnO3 films. Ceramics International, 2018, 44, 13695-13698. | 4.8 | 7 |
| 93 | Perovskite MAPb(Br1â^'Cl)3 single crystals: Solution growth and electrical properties. Journal of Crystal Growth, 2020, 549, 125869. | 1.5 | 7 |
| 94 | Low-temperature synthesis of (Pb,La)(Zr,Ti)O3 thick film on Ti substrates by the hydrothermal method using oxide precursors. Applied Physics Letters, 2006, 88, 012901. | 3.3 | 6 |
| 95 | Low-temperature growth of lead magnesium niobate thick films by a hydrothermal process. Ceramics International, 2008, 34, 1063-1066. | 4.8 | 6 |
| 96 | A Diagram of the Structure Evolution of Pb(Zn1/3Nb2/3) O3-9%PbTiO3 Relaxor Ferroelectric Crystals with Excellent Piezoelectric Properties. Crystals, 2017, 7, 130. | 2.2 | 6 |
| 97 | A Rapid, Label-free and Impedimetric DNA Sensor Based on PNA-modified Nanoporous Gold Electrode. International Journal of Electrochemical Science, 2017, 12, 10511-10523. | 1.3 | 6 |
| 98 | Large photoelectrochemical activity of flexible TiO2/SrRuO3 oxide heterojunction. Applied Surface Science, 2020, 504, 144544. | 6.1 | 6 |
| 99 | A novel protein binding strategy for energy-transfer-based photoelectrochemical detection of enzymatic activity of botulinum neurotoxin A. Electrochemistry Communications, 2018, 97, 114-118. | 4.7 | 5 |
| 100 | High-temperature ferromagnetic insulating phase in strained La0.8Sr0.2MnO3 thin films. Journal Physics D: Applied Physics, 2019, 52, 485001. | 2.8 | 5 |
| 101 | Structural and optical characteristics of the hexagonal ZnO films grown on cubic MgO (001) substrates. Optics Letters, 2016, 41, 4895. | 3.3 | 5 |
| 102 | Slow relaxation of piezoelectric response in CdZnTe ferroelectric semiconductor single crystals. Applied Physics Letters, 2007, 91, . | 3.3 | 4 |
| 103 | Morphotropic domain structures and dielectric relaxation in piezo-/ferroelectric Pb(ln1/2Nb1/2)O3–Pb(Zn1/3Nb2/3)O3–PbTiO3 single crystals. Journal of Crystal Growth, 2016, 441, 33-40. | 1.5 | 4 |
| 104 | Ferroelastic domain structure and phase transition in single-crystalline [PbZn1/3Nb2/3O3]1-x[PbTiO3]x observed via in situ x-ray microbeam. Journal of the European Ceramic Society, 2018, 38, 1488-1497. | 5.7 | 4 |
| 105 | Pulsed laser deposition of amorphous InGaZnO ₄ as an electron transport layer for perovskite solar cells. Journal of Advanced Dielectrics, 2019, 09, 1950042. | 2.4 | 4 |
| 106 | Realizing 60 GHz narrow-linewidth photonic microwaves with very low RF driving power. Laser Physics Letters, 2016, 13, 126202. | 1.4 | 3 |
| 107 | The flexoelectric transition in CaCu ₃ Ti ₄ O ₁₂ material with colossal permittivity. Journal of Applied Physics, 2022, 132, 024101. | 2.5 | 3 |
| 108 | Micro-Raman scattering and DC field dependent dielectric properties of BaZr x Ti 1 - x O 3 relaxor ferroelectric ceramics. Proceedings of SPIE, 2007, , . | 0.8 | 2 |

| # | Article | IF | CITATIONS |
|-----|--|-------------------|----------------------|
| 109 | A monolithically integrated photonic microwave generator. Laser Physics Letters, 2018, 15, 016201. | 1.4 | 2 |
| 110 | Negative Coriolis effect in piezoelectric metamaterials. Journal of Alloys and Compounds, 2019, 801, 262-266. | 5.5 | 2 |
| 111 | Effects of strain on ultrahigh-performance optoelectronics and growth behavior of high-quality indium tin oxide films on yttria-stabilized zirconia (001) substrates. Journal of Materials Science: Materials in Electronics, 2021, 32, 21462-21471. | 2.2 | 2 |
| 112 | Preparation and characterization of hydroxyapatite-polylactic acid HA-PLA composite film. Shenzhen Daxue Xuebao (Ligong Ban)/Journal of Shenzhen University Science and Engineering, 2016, 33, 10. | 0.2 | 1 |
| 113 | Visualization of Bubble Nucleation and Growth Confined in 2D Flakes (Small 39/2021). Small, 2021, 17, 2170205. | 10.0 | 1 |
| 114 | High-Temperature Flexible Transparent Heater for Rapid Thermal Annealing of Thin Films. Physical Review Applied, 2022, 17, . | 3.8 | 1 |
| 115 | Dielectric property of all-organic composite film composed of cobalt phthalocyanine and poly(vinylidene fluoride). , 2012, , . | | 0 |
| 116 | Structural and optoelectronic properties of combining Nb-doped SrTiO3/ITO films on (0 0 1)-YSZ substrate. Results in Physics, 2021, 26, 104436. | 4.1 | 0 |
| 117 | Glucose sensors based on solution-gated graphene transistors. Shenzhen Daxue Xuebao (Ligong) Tj ETQq1 1 0.7 | '84314 rgl 0.2 | 3T / Overlock |

Study on dielectric properties of hyperbranched zinc phthalocyanine. Shenzhen Daxue Xuebao (Ligong) Tj ETQq0 0.0 rgBT /Overlock 10